INNSPUB

RESEARCH PAPER   OPEN ACCESS

Synthesis and characterization of nanocomposite by using decolourization of dyes from aqueous solution

Swetha V, M. Petchiammal, G. Sabeena, E. Pushpalaksmi, J. Jenson Samraj, G. Annadurai*

Division of Nanoscience, Sri Paramakalyani Centre for Excellence in Environmental Sciences, Manonmaniam Sundaranar University, Alwarkurichi, India

Abstract
A series of biopolymer chitosan/montmorillonite nanocomposites were prepared by controlling the molar ratio of chitosan and montmorillonite. The nanocomposites were characterized by UV, FTIR, XRD, SEM, TGA, and FL analysis were performed to confirm the observed results. Batch adsorption experiments were carried out utilizing the composite to adsorb Congo red from aqueous solutions. As a result, increasing adsorbent dosage and initial dye concentration along with decreasing agitation speed, temperature, and initial pH led to increasing the amount of adsorbed Congo red. A rapid increment in the adsorption was happened with increasing adsorbent dosage from (1.0, 2.0 and 3.0g/L), pH (3.4, 5.8 and 9.4) and temperature (30ºC, 45ºC, and 60ºC) while further increment in the adsorbent dosage resulted in an insignificant increase in the adsorption (22.0, 24.0, 29.0,mg g^{-1}). The adsorption isotherms were also studied. It was shown that all the sorption processes were better fitted by the Langmuir and Freundlich isotherm equation. Moreover, the adsorption isotherm models were employed for the description of the Chitosan with montmorillonite nanocomposites dye adsorption processes. The antibacterial activity of Chitosan with montmorillonite nanocomposites showed more than 99% mortality against two Gram-negative bacteria and two Gram-positive bacteria. Because chitosan/montmorillonite nanocomposites could be recovered conveniently and possessed of excellent adsorptive property, it can be developed as an economical and alternative adsorbent to decolorize or treat dye wastewater.

*****Corresponding Author:** G. Annadurai ✉ gannadurai@msuniv.ac.in

Introduction

The field of nanotechnology is one of the most active areas of research in modern material sciences. Nanotechnology is a field that is developing day by day, making the impact in all spheres of human life and creating a growing sense of excitement in the life sciences especially biomedical devices and biotechnology (Jones *et al.,* 2008). Chitosan is the most abundant basic biopolymer and is structurally similar to cellulose, which is composed of only one monomer of glucose. Chitosan solubility, biodegradability, reactivity, and adsorption of many substrates depend on the amount of protonated amino groups in the polymeric chain, therefore on the proportion of acetylated and non-acetylated D-glucosamine units. The amino groups (pKa from 6.2 to 7.0) are completely protonated in acids with pKa smaller than 6.2 making chitosan soluble. Chitosan is insoluble in water, organic solvents, and aqueous bases and it is soluble after stirring in acids such as acetic, nitric, hydrochloric, perchloric and phosphoric (Guibal, 2007; Klug *et al.,* 1998 Kurita, 2006; Anthonsen and Smidsroed, 1995).

The unique character of nanoparticles for their small size and quantum size effect could make chitosan nanoparticles exhibit superior activities. Chitosan is the most cost-effective approach to prevent economic losses and morbidity caused by infectious diseases. The potential application of chitosan nanoparticles as a vaccine delivery has also been shown in numerous studies (Dutta *et al.,* 2004; Sridhari and Dutta, 2000). Montmorillonite is an aluminosilicate clay composed of tetrahedral layers of silica stacked between the octahedral layers of alumina. The isomorphous substitution of Al^{3+} for Si^{4+} in the tetrahedral layer and mg^{2+} for Al^{3+} in the octahedral layer results in a net negative surface charge on the clay. Montmorillonite has a large specific surface area and exhibits good adsorption, cation exchange, and drug-carrying capabilities (Khedr *et al.,* 2012). Mm Thas a large specific surface area and exhibits good adsorption ability, cation exchange capacity, standout adhesive ability, and drug-carrying capability. Thus, mm Tis a common ingredient as both the excipient and active substances in pharmaceutical products (Wang *et al.,* 2008). Montmorillonite (MMT) takes a layered structure consisting of an octahedral sheet of alumina or magnesia that is surrounded by two tetrahedral sheets of silica (Zhu *et al.,* 2011; Xia *et al.,* 2010). mm Tcan significantly improve thermal stability and mechanical properties when dispersed in a polymer matrix with low content, and exerts special behavior towards chemical species present in water and can also be used to fasten flocculation and improve the flake's textures (Assaad, *et al.,* 2007). CTS can be highly adsorbed or intercalated ontomm T. Wang and Wang, 2007, reported that CS/MMT improved the mechanical and material properties of Chitosan and additionally exhibited a higher adsorption capacity of anionic dyes when compared to CS andmmT. Kittinaovarat *et al.,* 2010, also reported that CS/MMT provided a higher adsorption capacity of reactive red, an anionic dye, compared to CS alone. However, a study of the removal of anionic dyes using CS/MMT as an adsorbent has not been documented. Chitin and chitosan have been inspected as an antimicrobial material against a broad range of target organisms like bacteria in experiments involving in vivo and in vitro cooperation with chitosan in different modes (solutions, films, and composites) Goy *et al.,* 2009.

The dispersibility and compatibility of antibacterials polymers are some of the key factors for the preparation of antibacterial polymers. To improve the compatibility between the antibacterial and polymer, surface modification of the antibacterial is required. Furthermore, a lot of researches (Lin *et al.,* 2018) shown that nanoparticles, such as clay and graphene nanoplatelets which were incorporated in antimicrobial polymer nanocomposites, allowed for the tuning of the release of antimicrobial agents, especially reducing the burst release effect, without hindering the antimicrobial activity of the obtained materials. However, the sprinkle reports on antibacterial studies of chitosan nanoparticle and chitosan nanocomposite established the efficiency of against various pathogenic microorganisms (Shiravand and Azarbani, 2017).

The present study was designed to prepare Chitosan (CS) and montmorillonite (MMT) polymer composites. In this study, Chitosan nanocomposites are synthesized by the precipitation method using montmorillonite and chitosan were investigated. We have focused on the preparation of Chitosan nanocomposite and their efficiency in the removal of dye from the congo red dye solution. The antibacterial activity of the chitosan with montmorillonite nanocomposites was evaluated

Materials and methods

All chemicals used in this study were of analytical grade and purchased from Merck, India, and used as obtained without additional purification. Stock solutions Congo red were prepared with distilled water. Required working solutions was obtained by suitable dilutions of the stock solutions by the addition of distilled water. Throughout the experiment, pH adjustments were carried out with 0.1N HCl or 0.1M NaOH as necessary.

Preparation of Chitosan Nanoparticle

1 gram of chitosan was weighed out and dissolved in 100ml of 1% acetic acid solution followed by continuous stirring at room temperature for about 1 hour by using a magnetic stirrer, and then 2g of sodium tripolyphosphate was dissolved in 200ml of distilled water and then added dropwise and freeze this solution in 40°C and 24hrs and then precipitate was settled at the bottom and collected the precipitate and dried hot air oven 50°C at 24hrs. Finally, was prepared the chitosan nanoparticle was investigated.

Preparation of chitosan with montmorillonite Nanocomposite

Chitosan Nanocomposite was prepared in a 1:1 ratio. Firstly, 1g of chitosan nanoparticle and then 1g of montmorillonite was mixed within 100ml distilled water and then this solution was shacked in shaken in 3 days. Next, the solution was filtered by using Whatman No: 1 filter paper. Finally, the particle was settled and then the particle was dried in a hot air oven at 24 hours, and then finally Chitosan with Nanocomposite was prepared.

Batch Equilibrium Studies

In batch equilibrium experiments, the Congo red dye solutions were prepared by dissolving the dye in deionized water to the required concentrations. A portion of adsorbent Chitosan with montmorillonite Nanocomposite of known (1g) and varied concentration of initial dye concentration 20-120mg/L was poured into the reaction conical flask. The time required to reach equilibrium as determined in equilibrium studies was 24h. The effect of adsorption isotherm was studied by carrying out a series of isotherm at different temperatures (30°C, 40°C and 60°C) and adsorbent dosages (1.0, 2.0, and 3.0g/L) and pH (3.4, 5.8, 9.4) respectively. The concentration of dye was measured with a UV-visible spectrophotometer.

Antibacterial Activity

The antibacterial activity of the chemical synthesized chitosan nanoparticle and Chitosan with montmorillonite Nanocomposite was determined by using the well diffusion method and then 5 types of bacteria were chosen. Antibacterial activity against the selected microorganisms was *Pseudomonas, Enterobacter, Escherichia coli* represented as Gram-negative bacteria while *Bacillus subtilis, Staphylococcus* represented as Gram-positive bacteria. Mueller-Hinton agar (MHA) and agar-agar were used for the cultivation of bacterial strains. The medium was sterilized by autoclaving at 121°C for 15 min. and then it was mixed well and poured into sterile Petri dishes (Reda Hassanien *et al.,* 2018).

Result and discussion

X-Ray Diffraction

XRD analysis revealed the nature of the Chitosan nanoparticle, Chitosan with montmorillonite Nanocomposite as shown in Fig 1 and 2. The XRD spectrum of the chitosan nanoparticles shows the synthesized Chitosan with montmorillonite Nanocomposite is crystalline nature.

The broad peaks of the XRD pattern may be due to the small size and incomplete inner structure of the particles stated that a high percentage of these

particles are amorphous. Hence XRD results confirmed that the synthesized materials are amorphous Chitosan Montmorillonite Nanocomposite. Similarly Noorsaiyyidah and Mohd, 2012).
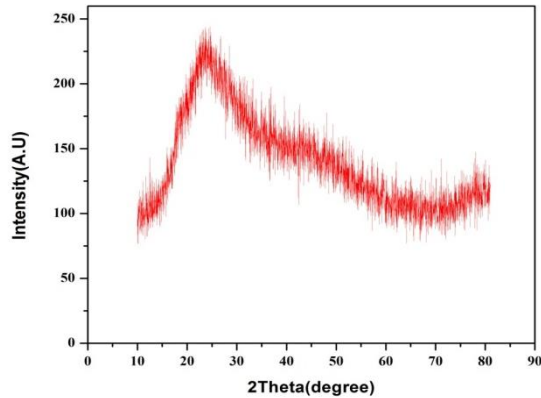

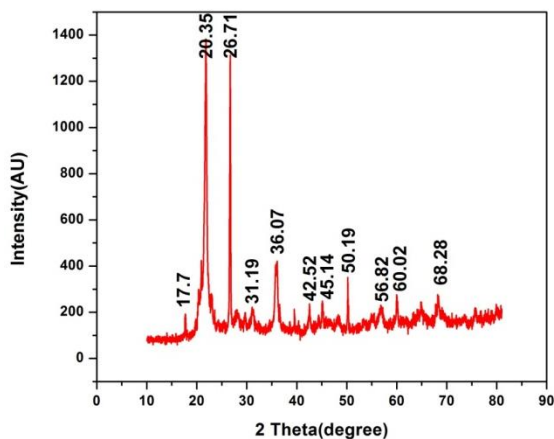**Fig. 1.** X-ray Diffraction (XRD) Analysis of Chitosan nanoparticle (CSNP).

Fig. 2. X-ray Diffraction (XR) Analysis of Chitosan with montmorillonite Nanocomposite

The XRD pattern clearly shows the synthesized chitosan nanoparticle and Chitosan with montmorillonite Nanocomposite formed are amorphous and crystalline. Fig 1, Shows the XRD patterns of Chitosan nanoparticle. Several strong Bragg reflections which correspond to the (20.35°), (26.71°), (36.07°), (42.52°), and (45.14°) reflections of chitosan nanocomposite Fig 2. The high intense peak for chitosan Nanocomposite is generally a reflection 2θ=20.35°, 26.71° which is observed in the sample. However, the broadening of the diffraction peaks indicates the presence of Chitosan with

montmorillonite Nanocomposite Fig 2. The XRD study indicates that the resultant particles are Chitosan with montmorillonite Nanocomposite. Many Bragg reflections corresponding to the (20.35°), (26.71°), (36.07°), and (42.52°) sets of lattice planes are observed that may be indexed based on the Chitosan with montmorillonite Nanocomposite.

Scanning Electron Microscopy
Scanning electron microscopy (SEM) pictures of CS Nanocomposite with various clay loadings are presented in Fig 3. Good and random dispersion ofmmT with various particle sizes in the CS matrix was observed. PolymermmT interaction, which leads to polar groups of clay and polymer, was also observed. However, pure CS has smooth surfaces. The smoothness of the surfaces is decreased by incorporating clay into the polymer matrix, and more clay resulted in more roughness. Interaction between clay and polymer matrix is also observed from the pictures. A small amount of clay resulted in more strong interaction than high-clay loadings Fig 3. This is because of the coagulation of the clay platelets in case of high-clay contents. Finally, both the dispersion of the clay in the polymer matrix and interaction between clay and polymer matrix were observed from SEM images (Harrison *et al.,* 2011). The particles in the Chitosan-MMT nano-composite display tight contact. A possible consequence of this layered structure is the improved retardation to deformation. This microstructure is correlated with the increase in elastic modulus and strength of chitosan composites prepared.
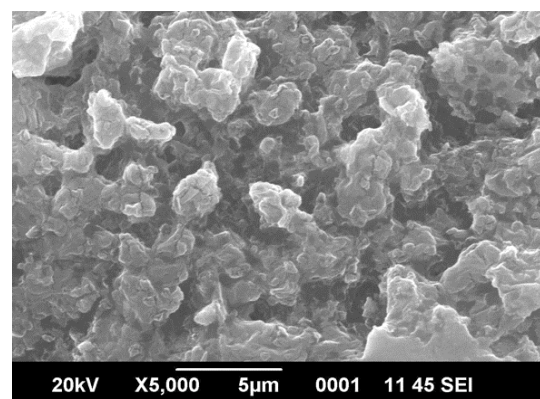

Fig. 3. Scanning Electron Microscopy analysis of chitosan nanocomposite.

Fourier Transform Infra-Red Spectroscopy

The FTIR technique was used to qualitatively analyze the interactions between functional groups in CS/MMT nanocomposite. To produce a biopolymer, chitosan was dissolved in 2% acetic acid solution. Analysis of the spectra measured in transmission mode Fig 4 and 5 shows that in the spectrum of CS/MMT. FT-IR has made this energy-limited region more accessible. It has made the middle infrared (400-4000cm⁻¹) also more useful. FT-IR studies were also conducted to investigate the structure of Chitosan nanoparticle (CSNP) and chitosan montmorillonite Nanocomposite (CSNC). The functional group of chitosan nanoparticle such as band at 2919cm⁻¹, 2853cm⁻¹ can be observed C-H Stretching bond and then 1600cm⁻¹ is C=O Stretching(acid) and then 1540cm⁻¹ can be observed C=C bond, 485cm⁻¹ is a Halogen compound [Iodo-compound] (C-I), 1480cm⁻¹ is a C-H Stretching, 1282cm⁻¹ which corresponds to C-N bond,1716cm⁻¹ can be observed C=O bond and then 601cm⁻¹ is –C- Cl bond. These are the functional group of the chitosan nanoparticle as shown in Fig 4. A band at 3324cm⁻¹2920cm⁻¹,2852cm⁻¹ corresponds to the combined peaks C-H, the vibration of C-O in alcohol hydroxyl group is present in at 1042cm⁻¹ and 1539cm⁻¹ can be represented as C=C bond and 1410cm⁻¹can be observed C-H Stretching bond, 720cm⁻¹ is presented as –C-H and then band at 600cm⁻¹ the can be represented as –C-Cl stretching bond, 558cm⁻¹ can be observed C-I bond, the peak at 420cm⁻¹ can be represented as alkyl halide (Katrin, *et al.,* 2017). These are the functional group of the chitosan with montmorillonite Nanocomposite as shown in Fig 5.
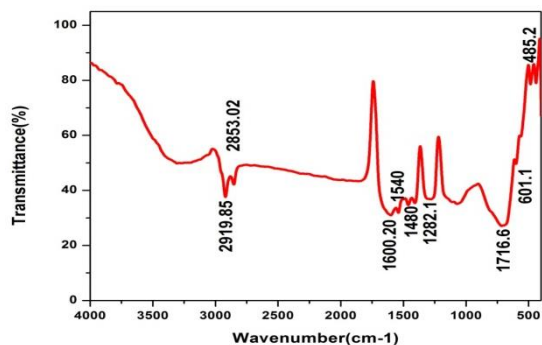

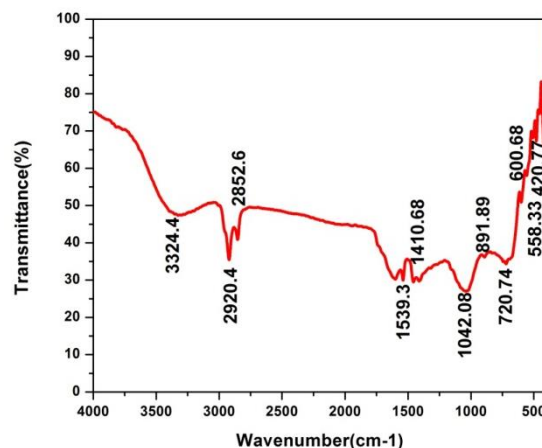**Fig. 4.** Fourier transforms infrared spectroscopy (FTIR Spectrum) Analysis of Chitosan Nanoparticle (CSNP).

Fig. 5. Fourier transforms infrared spectroscopy (FTIR Spectrum) Analysis of Chitosan with montmorillomite Nanocomposite (CSNC).

Differential thermal analysis (DTA)/ Thermogravimetric analysis (TG)

Thermal analysis is the analysis of a change in a property of a sample, which is related to an imposed change in the temperature. The sample is usually in the solid-state and the changes that occur on heating include melting, phase transition, sublimation, and decomposition.
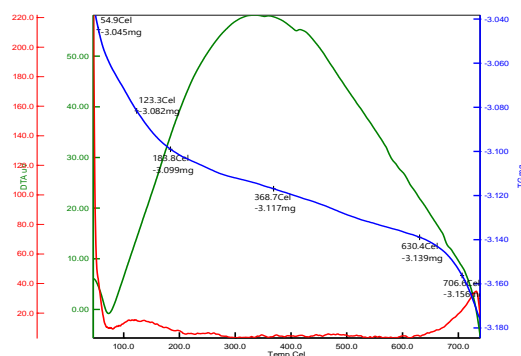

Fig. 6. TGA image of chitosan Montmorillonite Nanocomposite.

The DTA curve of Fig 6, shows a strong exothermic peak at 54.9 Cel (-3.045mg) probably corresponding to the lattice deformation of Chitosan or release of nitrate and acetate ion from chitosan with Montmorillonite Nanocomposite. Besides, two exothermic peaks were observed at 188.8 Cel (-3.099mg) and 630.4 Cel (-239mg) for chitosan with montmorillonite Nanocomposite (Fig .6). It may be due to sequential events of the lattice deformation

and release of the dopant ion, respectively. The corresponding weight loss is observed as shown in Fig 6, in TG curves. A similar result was observed [9] that when 50% weight loss was selected as a measuring point, CS/MMT nanocomposites with 2.5 wt% to 10 wt%mmT can be 25–1008C higher than that of pure CS.

Fluorescence spectroscopy

The fluorescence spectra of the chitosan nanoparticle were recorded at room temperature by Fluorescence spectrophotometer and it's shown in Fig 7. Intensities of maximum wavelength emissions were collected from the experiments seen in Fig 7 and the emission values were plotted as a wavelength Vs Intensity in Fig 7. For the sample of chitosan nanocomposite with the fluorescence intensity is getting increase exponentially by time. Although the saturation intensities are getting decrease with increasing monomer concentration were investigated. The fluorescence spectrum is a very useful technique for investigating energy levels (Katrin, *et al.*, 2017). The lower emission peak at 360 nm due to the radiating defects is related to the interface traps existing at the grain boundaries. The higher emission at 645 nm may also attribute to the surface defects and a few authors reported that these peaks are related to the dislocations or oxygen defects.
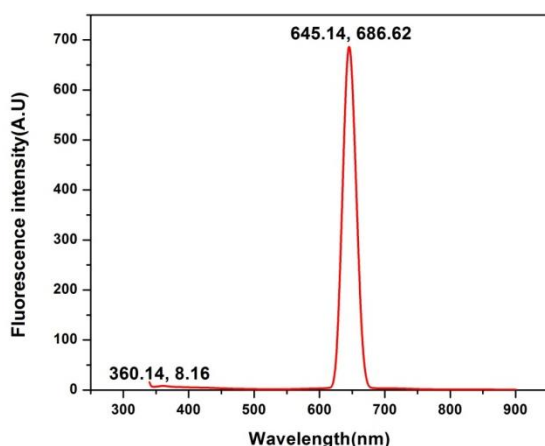

Fig. 7. Fluorescence image of chitosan nanoparticle.

Langmuir isotherm: The equilibrium adsorption isotherm is one of fundamental importance in the design of adsorption systems.

The isotherm expresses the relation between the mass of dye adsorbed at a particular dosage, temperature, and pH and liquid phase of dye concentration. For any adsorption investigation one of the most important parameters required to understand the behavior of the adsorption process in the adsorption isotherm.

The shape of an isotherm not only provides information about the affinity of the dye molecule for adsorption, but it also reflects the possible mode of adsorbing dye molecule. The most common way of obtaining an adsorption isotherm is to determine the concentration of dye solution before and after the adsorption experiments, although several attempts have been made to find the adsorbed amount. A basic assumption of the Langmuir theory [20] is that sorption takes place at specific sites within the adsorbent. The data obtained from the adsorption experiment conducted in the present investigation was fitted in different adsorbent dosage, temperature, and pH in the isotherm equation as shown in Fig 8-10. The optimum conditions for dye removal were identified and presented in a given table and graphs. The effect of the dose of adsorbent on equilibrium time was examined by conducting batch mode experiments with 40mg/L dye solution at the different pH at temperature with various doses of the adsorbent, namely 1.0 to 3.0g/L, respectively.

The agitation speed and the size of the adsorbent were kept conducting experiments (Langmuir, 1918). The study of the effect of the dose of adsorbent is necessary and very useful to find out the optimum amount of sorbent required for the removal of dye. The effect of adsorbent studies is observed from 5.0 to29.0mg/L as shown in Fig 8.

The amount of dye adsorbed increases with an increase in sorbent dosage due to the availability of more surface active sites for the adsorption of Congo red dye on the Chitosan with montmorillonite Nanocomposite. Initially, the rate of removal of dye is found to increase rapidly which slowed down as the dose increased.

The rate of adsorption is higher in the beginning as more free sites are available and unimolecular layers' increase, From the observed results the dose of adsorbent at 3.0g/L shows maximum removal of Congo red dye Fig 8 and after increase the dose of adsorbent there is no significant change. The pH of the solution is the dominant parameter in controlling the adsorption process onto the adsorbent (Prokop *et al.,* 2018). Hence, the influence of pH in the removal of dye was examined initially and the optimum pH for the adsorption of the dye on Chitosan with montmorillonite.

Nanocomposite was found effectively at pH 9.4 and a maximum of 24.0mg/L of the dye was desorbed at this pH as shown in Fig. 9. The amount of the dye adsorbed by the adsorbents decreases with an increase in temperature. The maximum amount of Congo red dye by the adsorbents decline from 5.0 to 24.0mg/L was studied as shown in Fig. 10. When the temperature was raised from 30 to 60ºC, the retardation in the extent of adsorbate is because at the higher temperature the solubility of adsorbate increases, and chemical potential decreases (Amidi *et al.,.,* 2011). As the temperature increases, the rate of diffusion of adsorbate molecules across the external boundary layer and interval pores of the adsorbent particles increases. Hence the change in the temperature will change the equilibrium capacity of the adsorbent for a particular adsorbate.

A plot of ($1/q_e$ vs $1/C_e$) resulted in a linear graphical relation indicating the applicability of the above model as shown in Fig 11-13. The Langmuir isotherm constants along with correlation coefficients are reported in Table 1.

$$q_e = \frac{KbC_e}{(1+bC_e)} \quad (1)$$

$$\frac{1}{q_e} = \frac{1}{K} + \frac{1}{KbC_e} \quad (2)$$

The various equations used for the isotherms (Eq 1-2). Batch mode adsorption studies were conducted and the effect of pH, dosages, and temperature in the adsorption process was studied using the adsorbent, Chitosan with montmorillonite Nanocomposite.

The values are calculated from the slope and intercept of the different straight lines representing the different dosages, pH, and temperature (b) energy of adsorption and (k) adsorption capacity. The Langmuir isotherm constant (b) in Eqn (1) is a measure of the amount of dye adsorbed when the monolayer is completed. Monolayer capacity (Q_m) of the adsorbent for the dye is comparably obtained from adsorption isotherm. The observed statistically significant (at the 95% confidence level) linear relationship as evidence of these by the R^2 values (close to unity) indicate the applicability of the isotherm (Langmuir isotherm) and surface.
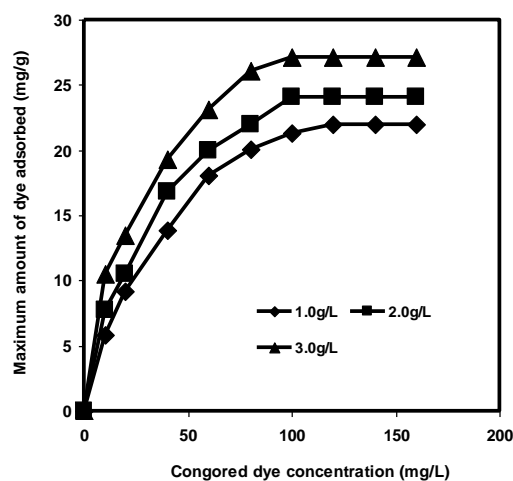

Fig. 8. Effect of specific dye uptake at different dosage (Chitosan-based with montmorillonite Nanocomposite) with Congo red dye concentration.
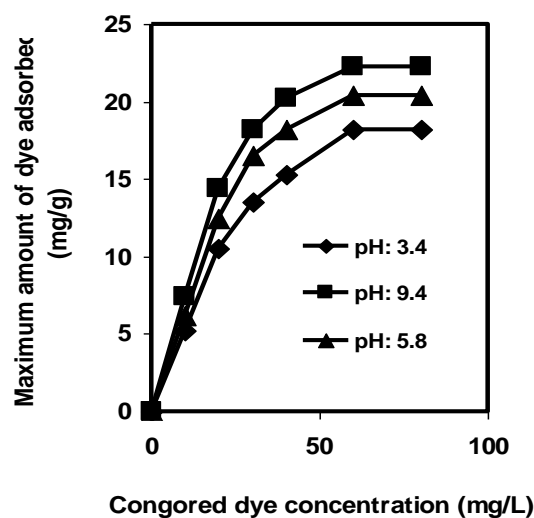

Fig. 9. Effect of specific dye uptake at different pH (Chitosan with montmorillonite Nanocomposite) with Congo red dye concentration.
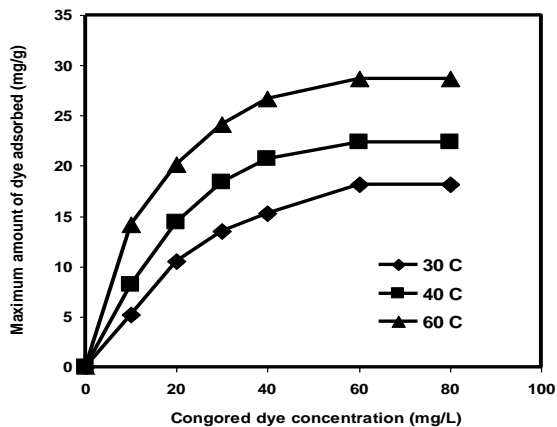
Fig. 10. Effect of specific dye uptake at different temperatures (Chitosan with montmorillonite Nanocomposite) with Congo red dye concentration.
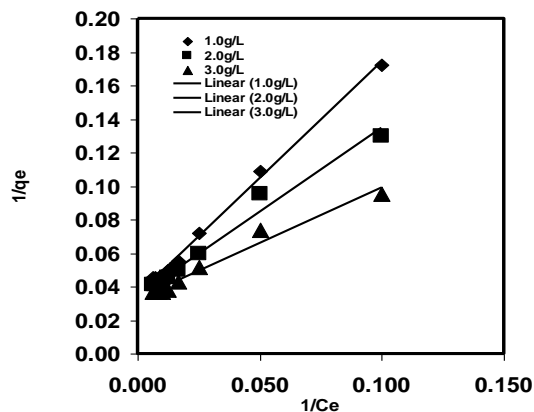

Fig. 11. Langmuir isotherm for the adsorption of dye using (Chitosan with montmorillonite Nanocomposite) at different adsorbent dosages with Congo red dye concentration.
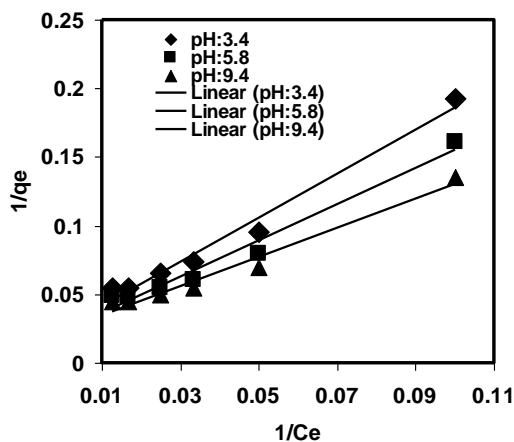

Fig. 12. Langmuir isotherm for the adsorption of dye using (Chitosan with montmorillonite Nanocomposite) at different pH with Congo red dye concentration.
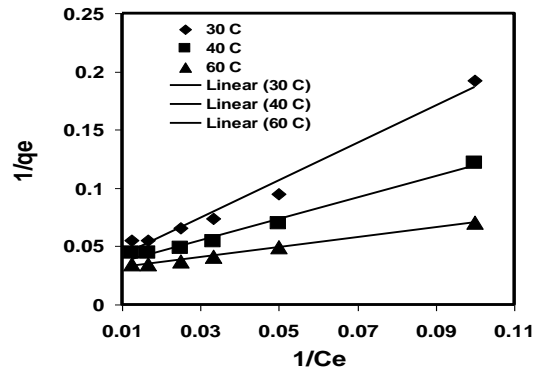

Fig. 13. Langmuir isotherm for the adsorption of dye using (Chitosan with montmorillonite Nanocomposite) at different temperatures with Congo red dye concentration.

Freundlich isotherm

Freundlich isotherm is used for heterogeneous surface energies systems. The sorption isotherm is the most convenient form of representing the experimental data at different dosages, pH, and temperature. The Freundlich equation, which was first used to describe gas phase adsorption and solute adsorption, is an empirical adsorption model that has been widely used in environmental chemistry.

$$q_e = K_F C_e^{1/n} \ (3)$$

$$\ln q_e = \ln K_F \, /(1/n) \ln C_e \ (4)$$

It can be expressed as Fig 14 to 16 as evidence of different binding sites, such interpretations are speculative. Where q and C were defined earlier, K_f is the distribution coefficient, and n is a correction factor. By plotting the linear form of Eq. (3-4), $\ln q_e = 1/n \ K_f \, /(1/n) \ln C_e$, the slope is the value of $1/n$ and the intercept is equal to log K_f. If $1/n = 1$, Eq. (3-4) becomes equal to Eq. (3-4) , and K_f is a partition coefficient. One of the major disadvantages of the Freundlich equation is that it does not predict an adsorption maximum.

The single K_f term in the Freundlich equation implies that the energy of adsorption on a homogeneous surface is independent of surface coverage. While researchers have often used the K_f and $1/n$ parameters to make conclusions concerning mechanisms of adsorption, and have interpreted multiple slopes from Freundlich isotherms (Assaad *et al.,* 2007).
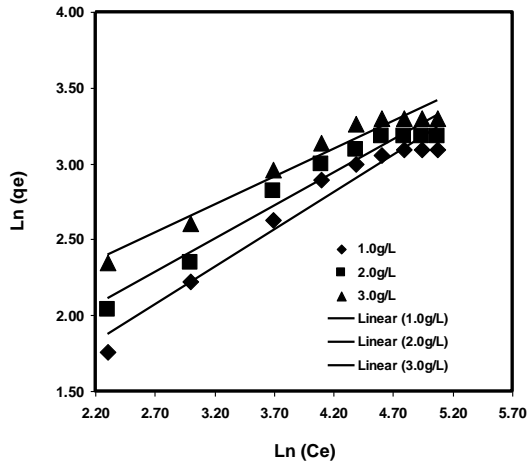
Fig. 14. Freundlich isotherm for the adsorption of dye using (Chitosan with montmorillonite Nanocomposite) at different adsorbent dosages with Congo red dye concentration.
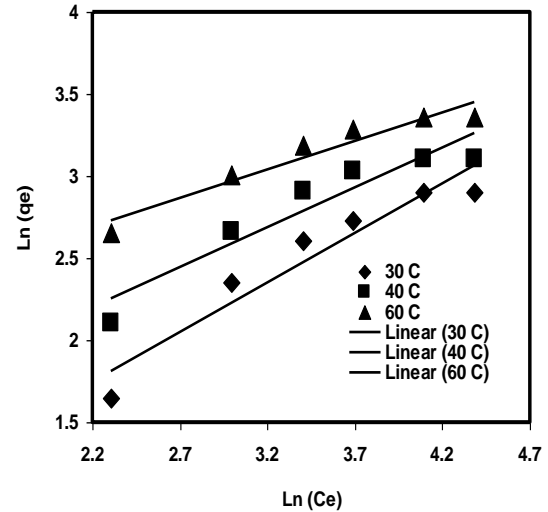

Fig. 15. Freundlich isotherm for the adsorption of dye using (Chitosan with montmorillonite Nanocomposite) at different pH with Congo red dye concentration.

Fig. 16. Freundlich isotherm for the adsorption of dye using (Chitosan with montmorillonite Nanocomposite) at different temperatures with Congo red dye concentration.
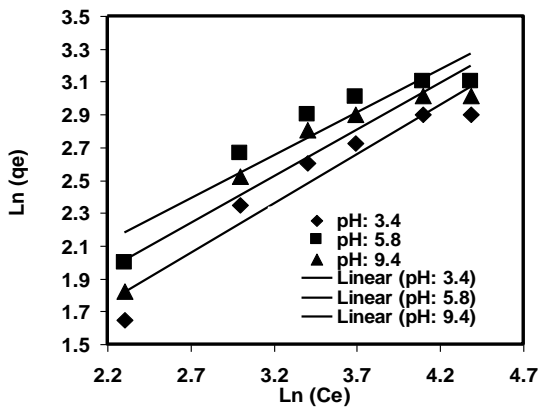
Antibacterial activity

In the first stage, the two different concentrations of chitosan nanoparticle and chitosan nanocomposite were prepared; 50µl and100µl sample powder was poured into the wells and the second stage of the Streptomycin antibacterial disc (Positive control) was used as a standard and then incubated at 37ºC for 24 has shown in Fig 17. These findings are shown in Table 2, Gram-positive bacteria, and gram-negative bacteria were most susceptible to synthesized chitosan nanoparticle and chitosan with montmorillonite Nanocomposite (Jaroniec, 1975).

Table 1. Langmuir and Freundlich isotherm constants at different dosage, temperature, and pH (Chitosan with montmorillonite Nanocomposite).

Parameters		Langmuir Isotherm -model parameters	Freundlich Isotherm -model parameters
Dosages (g/L)	1.0	KL=40.24; Qm=0072; R²=0.9968	Kf=0.7373; n=2.026; R²=0.9826
	2.0	KL=29.10; Qm=1.0; R²=0.9806	Kf=1.1089; n=2.30; R²=0.9532
	3.0	KL=20.45; Qm=1.50; R²=0.9720	Kf=1.555 n=1.91; R²=0.99539
Temperature (ºC)	30	KL=61.66; Qm=0.62; R²=0.9467	Kf=0.9732; n=1.76; R²=0.8926
	45	KL=58.64; Qm=0.72; R²=0.9805	Kf=0.8036; n=1.66; R²=0.8585
	60	KL=43.22; Qm=0.94; R²=0.9716	Kf=0.4286; n=1.45; R²=0.8574
pH	3.4	KL=32.99; Qm=1.09; R²=0.9829	Kf=0.3472; n=0.517; R²=0.8928
	5.8	KL=6165; Qm=0.67 R²=0.9806	Kf=0.4684; n=0.884; R²=0.8585
	9.4	KL=15.07; Qm=2.37; R²=0.9963	Kf=0.6021; n=2.36; R²=0.8754

Conclusions: The CS/MMT nanocomposites were prepared by controlling the molar ratios of CS tommT. The results show that the Congo red dye adsorption process is dependent on the molar ratios of CS/MMT, initial pH value of the dye solution, and temperature. The Langmuir isotherm and Freundlich isotherm follows the Langmuir monolayer model. Results obtained from this study showed that the

adsorption capacity of the nanocomposite for Congo red increased with increasing dosage, pH, and temperature. Introducing a small amount of mmT could improve the adsorption ability of the CS-MMT super adsorbent.

Table 2. Antibacterial activity of Chitosan nanoparticle and chitosan with montmorillonite Nanocomposite.

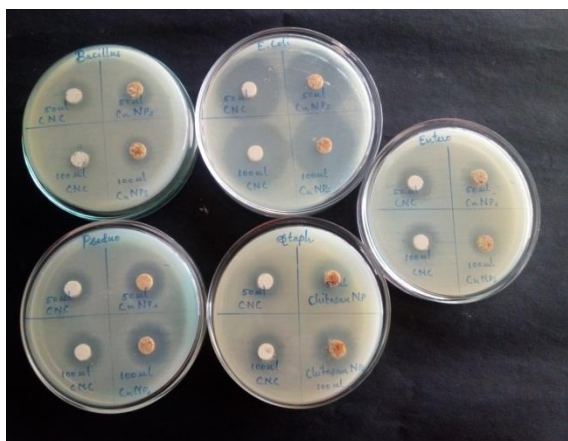| SN	Pathogens	Chitosan NPs Zone of inhibition inmm		Chitosan Nanocomposite Zone of inhibition inmm	
		50 µl	100 µl	50 µl	100 µl
1	*Bacillus subtillis*	21	20	17	20
2.	*E.coli*	31	32	37	39
3.	*Enterobacter*	20	21	15	22
4	*Pseudomonus*	21	22	15	20
5	*Staphylococcus*	20	22	19	21

Fig. 17. Antibacterial activities of Chitosan Nanoparticle and chitosan with montmorillonite Nanocomposite.

The equilibrium experimental data fit perfectly with the Langmuir isotherm. This indicates that the nanocomposite provided the potential for regeneration and reuse after Congo red dye adsorption. The investigated new material exhibits high adsorption capacity at a low concentration of dye and the very low mass of adsorbent and is more efficient than the other adsorbents used for removal of Congo red. As a result, it can be said that the chitosan withmmT nanocomposite is a very effective adsorbent for the removal of Congo red from aqueous solution. However, the sprinkle reports on antibacterial studies of chitosan nanoparticle and chitosan nanocomposite established the efficiency of various pathogenic microorganisms.

References

Amidi M, Romeijn SG, Borchard G, Junginger HE; Hennink WE, Jiskoot W. 2011. Preparation and characterization of protein-loaded N-trimethyl chitosan nanoparticles as nasal delivery system. J. Control. Rel **111,** 107-116,

Anthonsen MW, Smidsroed O. 1995. Hydrogen ion titration of chitosans with varying degrees of N-acetylation by monitoring induced 1H NMR chemical shift. Carbohydrate Polymers **26,** 303-305.

Assaad E, Azzouz A, Nistor D, Ursu AV, Sajin T, Miron DN, Monette F, Niquette P, Hausler R. 2007. Metal removal through synergic coagulation–flocculation using an optimized chitosan-montmorillonite system, Applied Clay Science **37,** 258-274.

Dutta PK, Dutta J, Tripathi VS. 2004. Chitin and chitosan: Chemistry, properties and applications. Journal of Scientific and Industrial Research **63,** 20-31.

Goy RC, Britto D, Assis OBG. 2009. A review of the antimicrobial activity of chitosan. Polímeros **19(3),** 241-247.

Guibal E. 2007. Interactions of metal ions with chitosan-based sorbents. A review. Separation and Purification Technology **38,** 43-74.

Harrison W, Erastus G, Paul K, Zhiyong T, Yan G. 2011. Synthesis silica nanoparticles with tunable physical properties by varying molar composition of reagents. Academic Journals **2,** 7-14.

Jaroniec M. 1975. Adsorption on heterogeneous surfaces: The exponential equation for the overall adsorption isotherm. Surface Science **50(2),** 553-564.

Jones N, Ray B, Ranjit KT, Manna AC. 2008. Antibacterial activity of ZnO nanoparticle suspensions on a broad spectrum of microorganisms. FENS Microbial Lett **279,** 71-76.

Katrin E, Sima S, Hossein M. 2017. Biosynthesis of copper nanoparticles using aqueous extract of *Capparis spinosa* fruit and investigation of its antibacterial activity. Marmara Pharmaceutical Journal **21(4),** 866-871.

Khedr MA, Waly AI, Hafez AAH. 2012. Synthesis of modified chitosan-montmorillonite nanocomposite. Aus. J. Basic App. Sci **6,** 216-226.

Kittinaovarat S. Kansomwan P. Jiratumnukul N. 2010. Chitosan/modified montmorillonite beads and adsorption Reactive Red 120. Applied Clay Science **48,** 87-91.

Klug M, Sanches MN, Laranjeiramc, Favere VT, Rodrigues CA. 1998. Análise das isotermas de adsorção de Cu(II), Cd(II), Ni(II) e Zn(II) pela N-(3, 4-dihidroxibenzil) quitosanaempregando o metodo da regressãonão linear. Quimica Nova **21,** 410-413.

Kurita K. 2006. Chitin and chitosan: Functional biopolymers from marine crustaceans. Marine Biotechnology **8,** 203-226.

Langmuir IJ. 1918. The adsorption of gases on plane surface of glass, mica and platinum. J. Chem. Soc. **40,** 1361-1364.

Lin Z, Jienan C, Wenji YU. 2018. Qingfeng Zhao and Jin Liu Antimicrobial Nanocomposites Prepared from Montmorillonite/Ag+/Quaternary Ammonium Nitrate. Journal of Nanomaterials **7,** 1-7.

Noorsaiyyidah D, Mohd R. 2012. Johan Complex Impedance Spectroscopy Study of Silica Nanoparticles Via Sol-Gel Method. International Journal of Electrochemical Science **7,** 5604-5615.

Prokop A, Kozlov E, Newman GW, Newman MJ. 2018. Water- based nanoparticulate polymeric system for protein delivery: permeability control and vaccine application. Biotechnology. Bioeng **78,** 459-466.

Reda Hassanien Dalal Z, Husein Mostafa F, Al-Hakkani A. 2018. Biosynthesis of copper nanoparticles using aqueous Tilia extract: antimicrobial and anticancer activities. Heliyon **4(1),** 7-7.

Shiravand S, Azarbani E. 2017. Phytosynthesis, characterization, antibacterial and cytotoxic effects of copper nanoparticles. Green Chem. Lett. Re **10,** 241-249.

Sridhari TR, Dutta PK. 2000. Synthesis and characterization of maleilated chitosan for dye house effluent. Indian J Chem Tech **7,** 198-204.

Wang L, Wang A. 2007. Adsorption characteristics of Congo Red onto the chitosan/montmorillonite nanocomposite. Journal of Hazardous Materials **147,** 979-985.

Wang X, Du Y, Luo J. 2008. Biopolymer/montmorillonite nanocomposite: preparation, drug-controlled release property and cytotoxicity. Nanotechnology **19,** 19-22.

Xia M, Jiang Y, Zhao I, Li F, Xue B, Sun M, Liu D, Zhang X. 2010. Wet grinding of montmorillonite and its effect on the properties of mesoporous montmorillonite. Colloids and Surfaces A: Physicochemical and Engineering Aspects **356,** 1-9.

Zhu S, Chen J, Zuo Y, Li Y. 2011. Cao, Montmorillonite/polypropylene nanocomposites: Mechanical properties, crystallization and rheological behaviors. Applied Clay Science **52,** 171-178.